Materials Today Bio 23 (2023) 100836

Contents lists available at ScienceDirect

Materials Today Bio

journal homepage: www.journals.elsevier.com/materials-today-bio

Biomimetic nanoplatform with anti-inflammation and neuroprotective effects for repairing spinal cord injury in mice

Xuechen Yin [a,1], Sen Lin [b,1], Ying Xiong [c], Peng Zhang [b,**], Xifan Mei [b,*]

[a] Department of Laboratory Medicine, Third Affiliated Hospital of Jinzhou Medical University, Jinzhou, China
[b] Department of Orthopedic, Third Affiliated Hospital of Jinzhou Medical University, Jinzhou, China
[c] Normandie Université, ENSICAEN, UNICAEN, CNRS, Laboratoire Catalyse et Spectrochimie (LCS), France

ARTICLE INFO

Keywords:
Biomimetic nanoplatform
Spinal cord injury
Polarization
Immunoengineering
Neuroinflammation

ABSTRACT

Regeneration in the therapeutics of spinal cord injury (SCI) remains a challenge caused by the hyper-inflammation microenvironment. Nanomaterials-based treatment strategies for diseases with excellent therapeutic efficacy are actively pursued. Here, we develop biodegradable poly (lactic-*co*-glycolic acid) nanoparticles (PLGA) obtained by loading celastrol (pCel) for SCI thrapy. Cel, as an antioxidant drug, facilitated reactive oxygen species (ROS) scavenging, and decreased the generation of pro-inflammatory cytokines. To facilitate its administration, pCel is formulated into microspheres by oil-in-water (O/W) emulsion/solvent evaporation technique. The constructed pCel can induced polarization of macrophages and obviously improved lipopolysaccharide (LPS) and interferon-γ (IFN-γ)-induced mitochondrial dysfunction, and increased neurite length in PC12 cells and primary neurons. In vivo experiments revealed that pCel regulated the phenotypic polarization of macrophages, prevented the release of pro-inflammatory cytokines, promoted myelin regeneration and inhibited scar tissue formation, and further improve motor function. These findings indicated that the neuroprotective effect of this artificial biodegradable nanoplatform is benefit for the therapy of SCI. This research opens an exciting perspective for the application of SCI treatment and supports the clinical significance of pCel.

1. Introduction

Recently, the number of patients with traumatic spinal cord injury (SCI) has been increasing globally, and this disease can seriously affect their motor function [1–3]. In the pathological process of SCI, it is generally accompanied by excessive generation of reactive oxygen species (ROS), inflammation, and secondary damage to the central nervous system (CNS), which has a negative impact on the treatment of such patients [4,5]. ROS is closely related to cell activity, and research has found that it can affect cell proliferation, survival, apoptosis levels, and is also related to cell resistance [6]. Therefore, during the treatment of SCI, clearing ROS and reconstructing the microenvironmen in the injured spinal cord are the focus of research. However, the difficulty of controlling ROS is increasing, and there are still many issues that need to be further studied.

Nanoplatform with enzyme-like structures and functions can regulate ROS levels in cells through catalytic activation pathways derived from immune cells, thereby providing support for the treatment of SCI related diseases [7,8]. Poly (lactic-*co*-glycolic acid) (PLGA) is a high-performance polyester polymer that is biodegradable [9]. At present, in the field of drug carrier research, PLGA-based nanoplatforms have attracted attention due to their performance advantages, such as low toxicity, high drug loading, and drug release potential [10,11]. In this nanoplatform, drugs can be slowly released, thereby significantly improving the therapeutic effect of drugs. In addition, PLGA-based nanoplatforms can be designed with convenient size, active site, which can efficiently target to specific cells and also help improve drug efficacy [12,13].

Celastrol (Cel) is an antioxidant and also has a certain inhibitory effect on inflammatory reactions [14–16]. Cel can promote the polarization of M1 to the M2 phenotype and play a regulatory role in the balance of immune response [17]. However, previous studies have found that the degradation and poor solubility of this drug under physiological conditions. Considering the ROS-enriched condition of

* Corresponding author
** Corresponding author
E-mail addresses: 1758016017@qq.com (P. Zhang), meixifan@jzmu.edu.cn (X. Mei).
[1] Xuechen Yin and Sen Lin Contributed equally to this work.

https://doi.org/10.1016/j.mtbio.2023.100836
Received 31 May 2023; Received in revised form 7 October 2023; Accepted 14 October 2023
Available online 10 November 2023

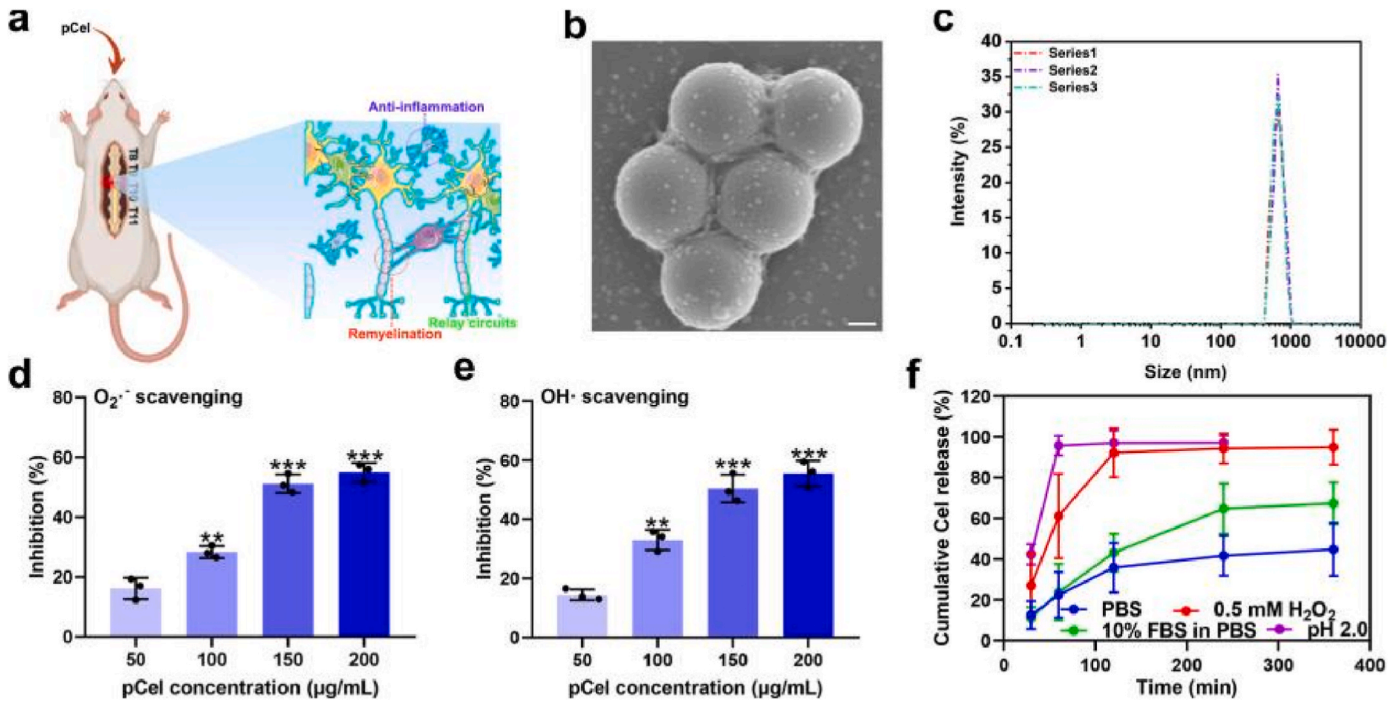

Fig. 1. Characterization of the pCel. (a) Scheme of pCel-based therapy for SCI. Scale bar = 200 nm. (b) TEM results of pCel. (c) DLS of pCel. (d) O^{2-} scavenging activities of pCel. (e) ·OH scavenging activities of pCel. (f) Cumulative Cel release analysis of pCel. **P < 0.01, ***P < 0.001.

injured spinal cord and poor solubility of Cel, a novel nanoplatform delivery system with Cel (pCel) was established by using PLGA. pCel were optimized to rebuild the microenvironment (Fig. 1a). The evaluation of ROS scavenging-driven SCI therapy was conducted based on LPS and IFN-γ inducing BV2 cells and spinal cord contusion mice. The pCel not only effectively eliminated ROS and polarized M1 toward M2 phenotype, but also promoted function recovery and hindered scar tissue hyperplasia. Importantly, pCel drastically decreased the mortality and alleviated the motor dysfunction via preventing pro-inflammatory cytokines and ROS level. With higher biocompatibility, pCel administration can be regarded as a excellent agent inhibiting ROS-associated neuroinflammation.

2. Results and discussion

2.1. Preparation and characterization of pCel

In the experimental process, two phases were first prepared; The oil phase consists of dichloromethane (DCM) (5 mL), Cel (50 mg), and Resomer ® RG 502H (400 mg) is composed, while the aqueous phase is relatively simple and consists solely of PVA solution (1 % w/v). Prepare 0.1 % (w/v) polyvinyl alcohol (PVA) culture medium (50 mL) according to experimental requirements. The internal phase is prepared by dissolving polymers and drugs through vortex stirring. Then, the aqueous phase was added to the organic phase at a suitable speed, and the O/W lotion was produced at 8000 rpm after full agitation. The resultant emulsion was later added to the maturation medium for 3 h, in an incubation bath at 40 °C under magnetic stirring (100 rpm) to ease the organic solvent evaporation. pCel were then collected by filtration through a 25 μm nylon sieve and a 10 μm nylon filter respectively, to select the desired size interval.

As shown in the TEM results (Fig. 1b), the pCel microspheres are spherical and exhibit a good solid structure. From Fig. 1c, it can be observed that the average particle size of this microsphere is about 720 nm, with high particle size concentration. Select typical free radicals ROS, O^{2-}, and ·OH for experimental research, and analyze the ROS-scavenging effect of pCel. According to Fig. 1d and e, pCel exhibits high ROS scavenging activity, and the scavenging performance is positively correlated with concentration. After pCel treatment, 55 % of the total O^{2-} is 150 μg/mL pCel clearance (Fig. 1d). About 58 % of the ·OH was decomposed after treated by 150 μg/mL pCel (Fig. 1e). To deeply verify the anti-oxidative effect of pCel, a ROS scavenging experiment was tested by classic 2,2′-azino-bis (3-ethylbenzothiazoline 6-sulfonate) (ABTS) radical assay. As exhibited in Supplementary Figure 1, about 70 % of free radical were eliminated by pCel (100 μg/mL). Moreover, no significant changes were observed in the zeta potential of pCel following 7 days of storage in different solution at 37 °C, indicating that these particles were highly stable (Supplementary Figure 2). Furthermore, the cumulative Cel release amount of pCel was tested to evaluate the release behavior under different pH conditions (Fig. 1f). Compared with releasing only ~40 % of Cel in PBS at 6 h and only ~60 % of Cel in PBS solution (10%FBS) at 6 h, the release rate of pCel was increased to ~95 % and ~98 % in 0.5 mM H_2O_2 and PBS solution (pH = 2.0), respectively. The property from oral delivery of pCel is mainly ascribed to the accelerated dissociation of Cel in ROS-enriched microenvironment. Thus, these results demonstrated that pCel has higher ROS-scavenging effect.

2.2. pCel polarized M1 macrophages toward M2 in vitro

To confirm the macrophages reprogramming of the pCel polarization of macrophages by marking interleukin-1β (IL-1β, red, M1 marker) and Arg-1 was observed in Fig. 2a (left). LPS + IFN-γ-treated macrophages showed M1 phenotype, and Cel restricted M1 polarization (Fig. 2a right). The macrophages expressed lower red signal in pCel group, which showed that pCel significantly inhibited the M1 polarization. The fluorescent result indicated that the level of IL-1β-positive macrophages decreased treated with Cel for 6 h, while those of Arg-1-positive macrophages increased (Fig. 2b and c). A significant improvement of Arg-1-positive macrophages was found in pCel group. The M1 ratio in LPS + IFN-γ group approximately reached 45 %, further indicating that pCel can prevent inflammatory response and promote M2 polarization. Moreover, after re-treated with LPS + IFN-γ (M2* cells), pCel group had a much higher Arg-1 and lower IL-1β fluorescence (Fig. 2d). These data

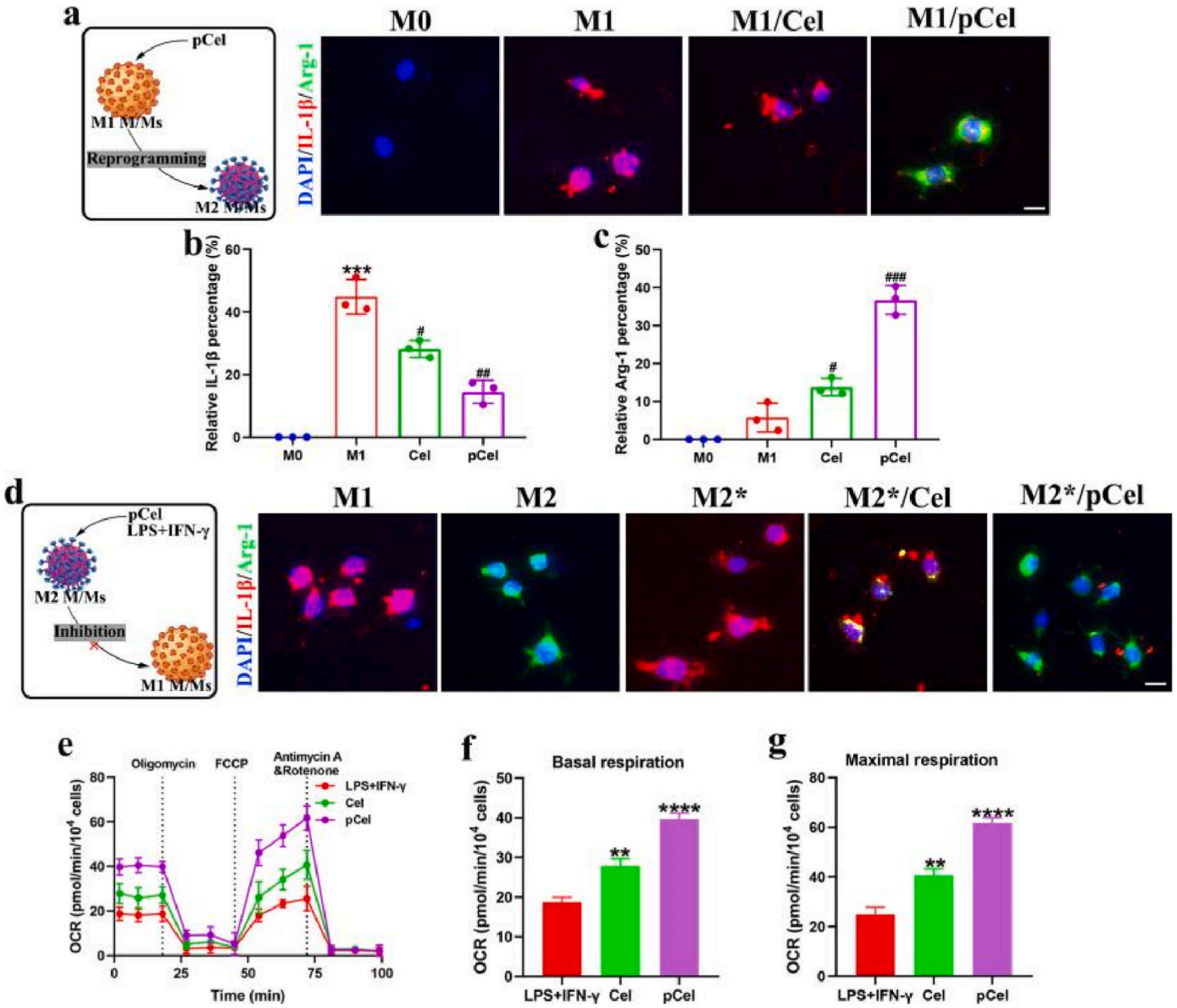

Fig. 2. Macrophage polarization of pCel. (a) Scheme for M1-M2 polarization by pCel (left) and typical images of IL-1β- and Arg-1-marked cells (right). (b, c) Representative quantification of marker intensity in cells treated with pCel. ***P < 0.001, compare to M0 group. #P < 0.05, ###P < 0.001, compare to LPS + IFN-γ group. (d) Scheme for inhibition of polarization by pCel (left) and typical images of the marked cells (right). (e) Seahorse mitochondrial stress tests of LPS + IFN-γ-caused macrophages treated with pCel, Cel or PBS. (f) Representative analysis of basal respiration in LPS + IFN-γ-induced macrophages treated with pCel, Cel or PBS. (g) Representative analysis of maximal respiration in LPS + IFN-γ-induced macrophages treated with pCel, Cel or PBS. Scale bar = 10 μm **P < 0.01, ***P < 0.001, ****P < 0.0001, compare to LPS + IFN-γ group.

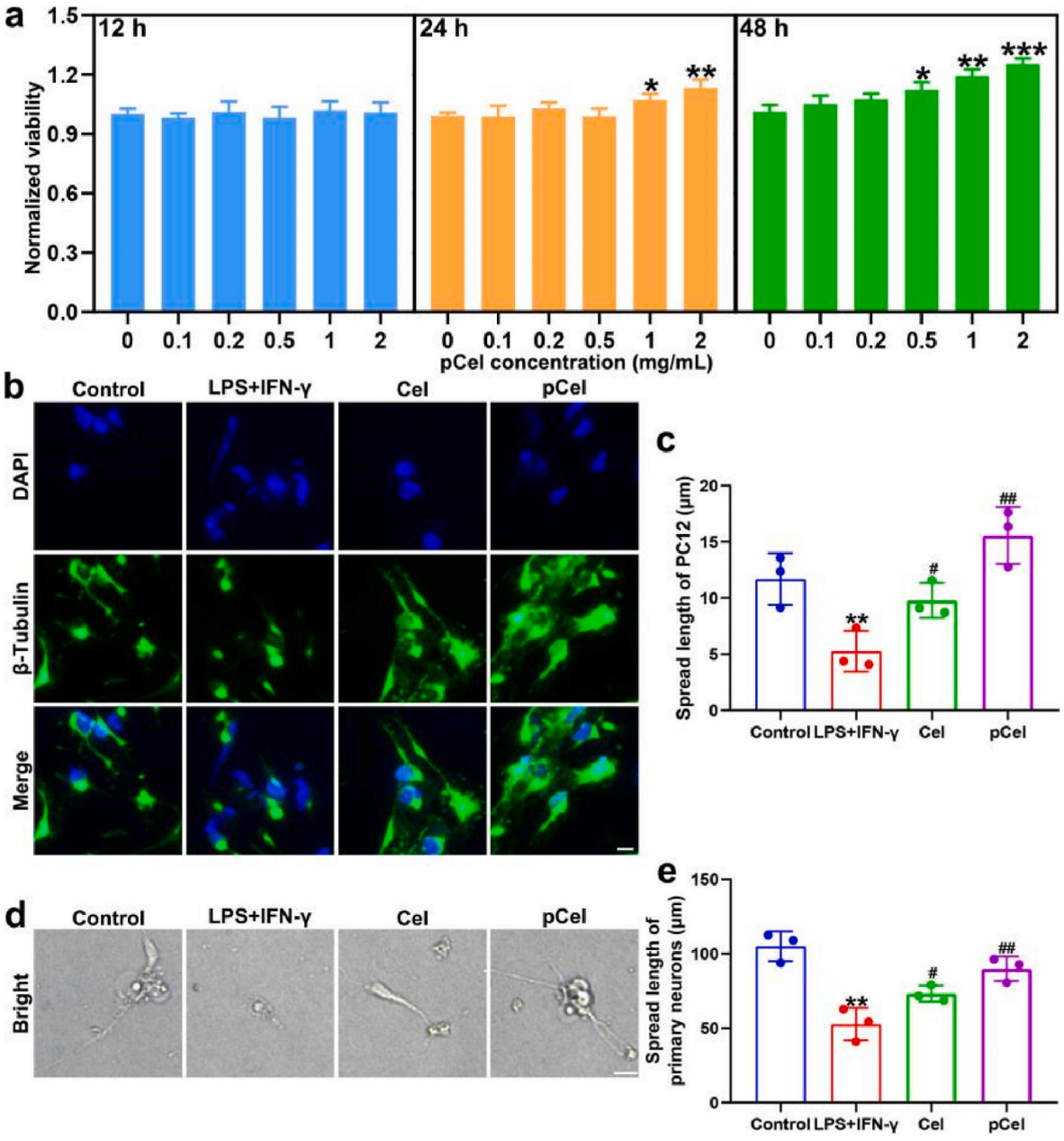

Fig. 3. pCel effected the proliferation. (a) Neuronal viabilities test of pCel. *P < 0.05, **P < 0.01, ***P < 0.001. (b) Representative images of neurite outgrowth in LPS + IFN-γ-induced PC12 cells treated with pCel, Cel or PBS. Scale bar = 10 μm. (c) Representative quantification of neurite outgrowth in LPS + IFN-γ-induced PC12 cells treated with pCel, Cel or PBS. (d) Representative images of neurite outgrowth in induced primary neurons treated with pCel, Cel or PBS. Scale bar = 50 μm. (e) Representative quantification of neurite outgrowth in LPS + IFN-γ-induced neurons treated with pCel, Cel or PBS. **P < 0.01, compare to control group; #P < 0.05, ##P < 0.01, compare to LPS + IFN-γ group.

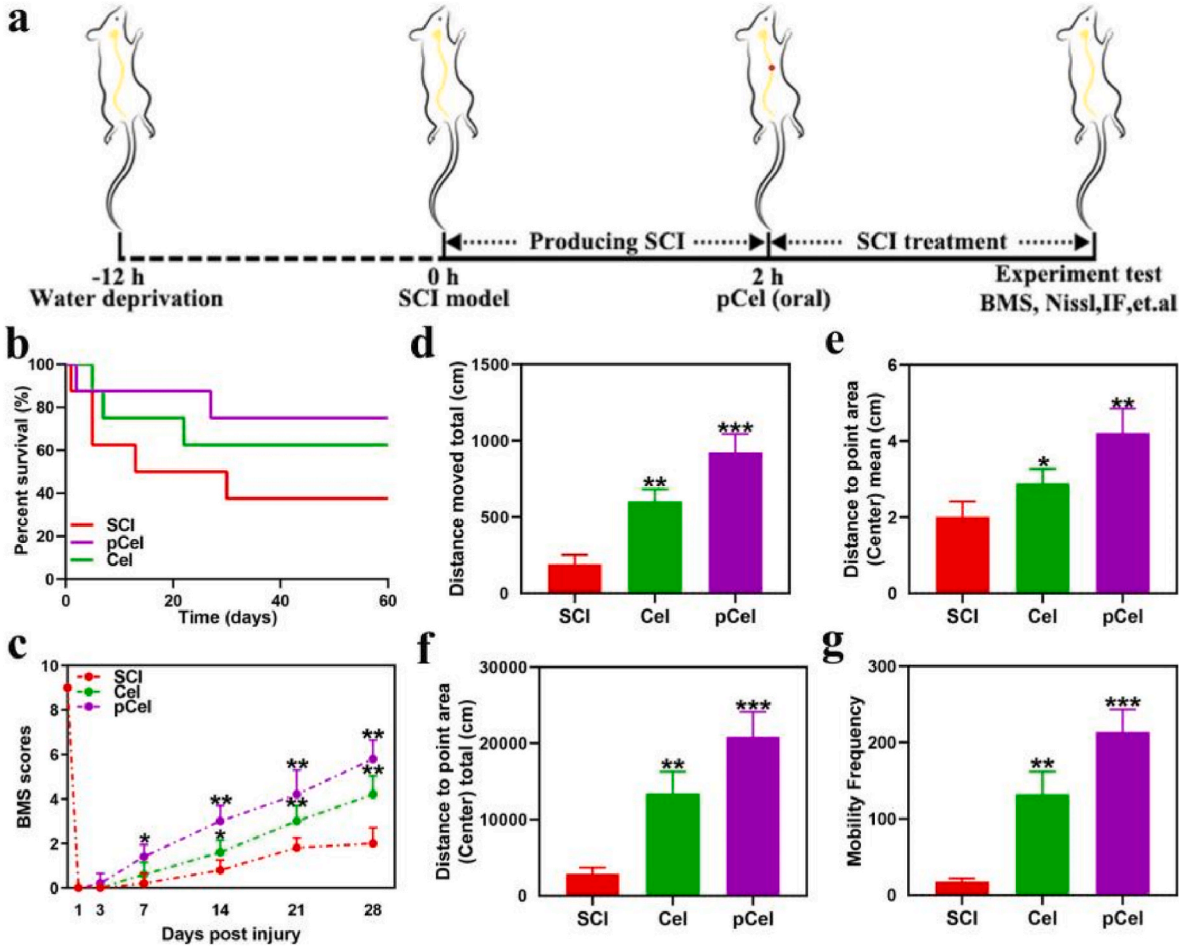

Fig. 4. In vivo treatment effects of pCel in SCI mouse. (a) The corresponding bioefficacy assay. (b) Survival curves of research objective with various therapy. (c) BMS scores of SCI mice. (d–g) the total distance moved, distance to point area mean, as well as mobility frequency in SCI mice. *P < 0.05, **P < 0.01, ***P < 0.001, compare to SCI group.

showed that macrophages induced by LPS + IFN-γ were in the inflammatory state, and this effect was significantly inhibited by pCel.

We next tested the ability of pCel to drive metabolic reprogramming. As shown in Fig. 2e–g, we found that compared with the LPS + IFN-γ group, the OXPHOS level of pCel-treated cells was significantly increased. According to the above experimental research, pCel exhibits a significant inhibitory effect on inflammatory responses in M1 macrophages, while also having a certain regulatory effect on metabolism.

2.3. pCel effected the proliferation and neurite outgrowth

Neurons play an extremely important role in function recovery after SCI. The cytocompatibility of pCel was assessed based on detectingimpact on the activity of PC12 cells (Fig. 3a). No obvious cytotoxicity was observed for pCel within the concentration range (0.1−2.0 mg/mL) and the tested time (12−48 h). Increased neuron activity appeared after treating with pCel for 24,48 h. After 24 h administration, higher neuron viability increase was detected under condition of pCel (2.0 mg/mL). While the treatment time reached 48 h, the concentration as low as 0.5 mg/mL caught a significant neurons viability improvement. These data showed the neuroprotective influence of pCel in vitro.

The LPS + IFN-γ decreased neurite elongation in PC12 cells (approximately 5 μm). The neurite elongation in the Cel (approximately 10 μm) and pCel (approximately 16 μm) groups was higher compared to that in LPS + IFN-γ group (Fig. 3b and c). Moreover, a similar effect was found in primary neurons (Fig. 3d and e). Therefore, pCel can form proper niche to induce the proliferation of neural cells.

2.4. pCel enhanced SCI mice motor ability

To assess the in vivo therapy of pCel, they were orally delivered into spinal cord transection model mice (Fig. 4a). The animals in the SCI, Cel, and pCel groups faced paralysis over 2 months, whereas significant motor function restoration was observed in the pCel group. The results showed that the survival rate of mice was significantly improved after treatment with Cel and pCel (Fig. 4b). The improvement effect of pCel on behavioral function was evaluated by the Basso Mouse Scale (BMS). The results showed that the behavioral function of mice was significantly improved after pCel treatment (Fig. 4c). An open field test (OFT) was used to further investigate the activity of mice. The analysis shows that compared to other groups, the pCel group had a significantly higher total distance moved, distance to point area mean, distance to point area, and mobility frequency than the other groups (Fig. 4d–g). Furthermore, we detected the pCel concentration of 5287.7 ± 1962.3 ng/g in the T9-T10 injured spine cord by Gas Chromatography-Mass Spectrome (GC-MS). To deeply assess the treatment efficacy of pCel, the number of neurons and the size of gilal scar was tested (Supplementary Figure. 3, 4). pCel group significantly improved neurons surviving in ventral anterior horn and decreased lesion in dorsal injured spinal cord. These data demonstrated that pCel can obviously enhance the function ability of mice.

2.5. pCel effected M1 macrophage to M2 phenotype at the injured lesion

The phenotype of macrophages exhibits various capability to exert

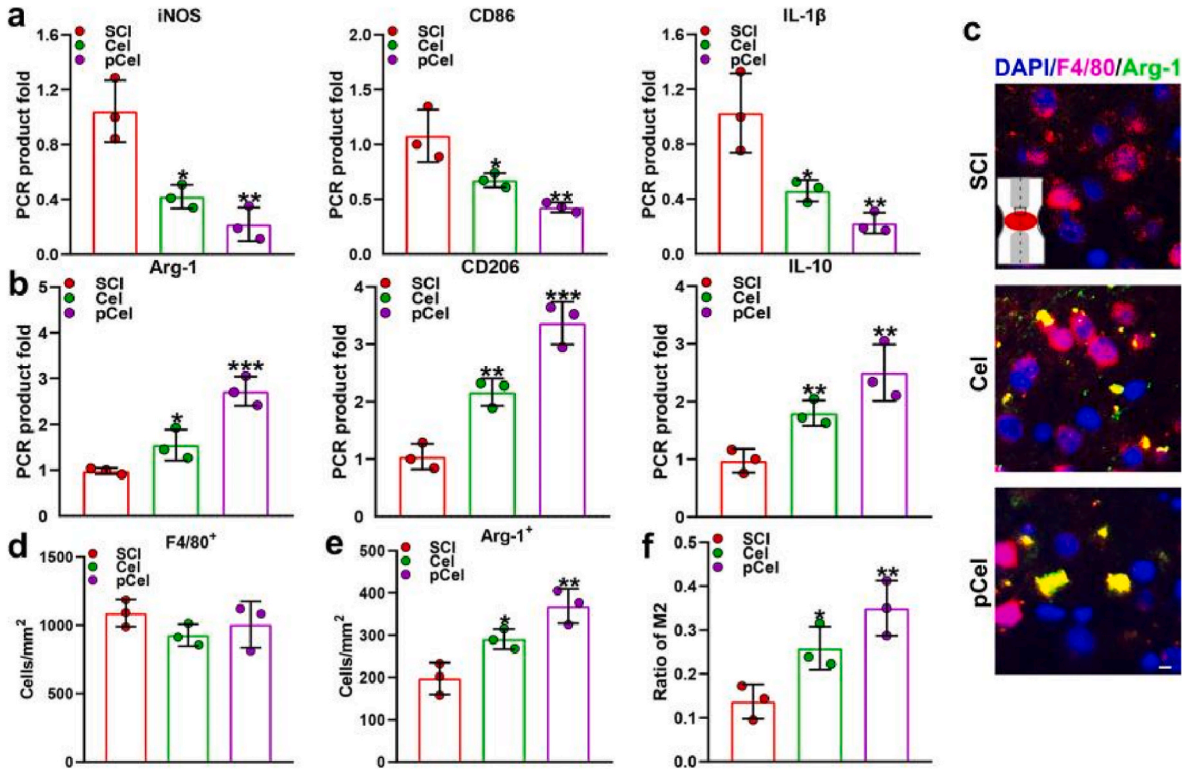

Fig. 5. The macrophages polarization of pCel. (a) typical result of mRNA levels of iNOS, IL-1β. (b) Result of mRNA levels of Arg-1, CD206. (c–f) typical images and result of colocalization. Scale bar = 10 μm *P < 0.05, **P < 0.01, ***P < 0.001, compare to SCI group.

functions in SCI. M1 macrophages, highly labeled inducible nitric oxide synthase (iNOS), CD86 and interleukin-1β (IL-1β), have cytotoxic effect on SCI. As highly expressed arginase-1 (Arg-1), CD206, interleukin-10 (IL-10), M2 macrophages can promote regeneration and inhibit inflammation after SCI. The analysis of markers for M1 and M2 macrophages in the injured spinal cord showed that the mRNA levels of iNOS, CD86 and IL-1β in pCel group were significantly lower than those in other groups (Fig. 5a). As key markers of M1 phenotype, these genes are related to inflammatory response and the release of proinflammatory cytokines, and contribute to the hyperinflammation microenvironment in the lesion. In contrast, the mRNA levels of Arg-1, CD206 and IL-10 in pCel group were significantly increased as compare to SCI and Cel groups (Fig. 5b). Subsequently, these data were tested to quantify the total number of Arg-1+cells (DAPI+/CD206+), macrophages (DAPI+/F4/80+) and M2 macrophages (DAPI+/F4/80+/CD206+) on the 7th day after SCI (Fig. 5c). Total number of infiltrated macrophages in these group was indifference (Fig. 5d). Moreover, compared with SCI group, the number of Arg-1+ cells in Cel and pCel significantly increased (Fig. 5e). In addition, in the pCel group, the ratio of M2 phenotype to the total number of macrophages was significantly increased 3-fold as compare to SCI group (Fig. 5f). Therefore, these data demonstrated that pCel polarized M1 macrophages toward M2 and inhibited inflammation response in acute SCI.

2.6. pCel effected the synaptic regeneration and scar generation via inhibiting neuroinflammation

Spinal cord regeneration includes scar hyperplasia, and synaptic reconstruction [18–20]. Next, we studied the regenerative effect of pCel administration at the beginning of the chronic phase of SCI (on the 28th day after SCI). The fluorescence intensity of CSPGs in the pCel group was significantly lower than that of the other groups, indicating that there were fewer scar tissues at the injury site (Fig. 6a and b). In addition, abundant synapse (Syn) is critical for nerve regeneration and axon extension. An increased syn signal in the peripheral region was observed after treatment with pCel (Fig. 6c and d). Compared with SCI group, pCel administration significantly increased the number of myelinated axons (Supplementary Figure 5). The expression of proteins associated with neuronal and glial scar was comparable in the SCI and Cel groups, demonstrating that pCel were favorable for the effective treatment of CNS-related diseases. Furthermore, after pCel feeding, the level of TNF-α, IL-1β and IL-6 significantly decreased on day 7 post-SCI (Fig. 6e, Supplementary Figure 6, 7). Thus, the inhibition of inflammation at the early stage of SCI could be decreased, and an environment for the induced regeneration of the spinal cord could be created at late stage of SCI.

Cel Administration leads to hematological and liver toxicity, which limits the further application of Cel. The data exhibited no obvious difference in both pCel and normal group (Supplementary Figure 8-12). These finding showed that the pCel had no obvious long-term side effects in vivo.

In fact, Thefollowing mentioned nanomedicine prevented further destruction of SCI, but there are still many shortcomings, as shown in Table 1. All these findings suggested that anti-inflammatory targeted therapies may play an important role in the treatment of SCI. Compared with the various previously reported drugs, pCel has a better therapeutic effect on SCI rats because the damage recovers faster (Table 1).

3. Conclusion

In summary, we developed pCel to investigate their therapeutic effects as novel nanoplatform for SCI. pCel polarized M1 macrophages to M2 and promoted neurite outgrowth in vitro, demonstrating the synergistic treatment strategy for neuro-associated cells under pathological conditions. The in vivo results revealed that pCel regulated the macrophages polarization, inhibited the release of proinflammation cytokines,

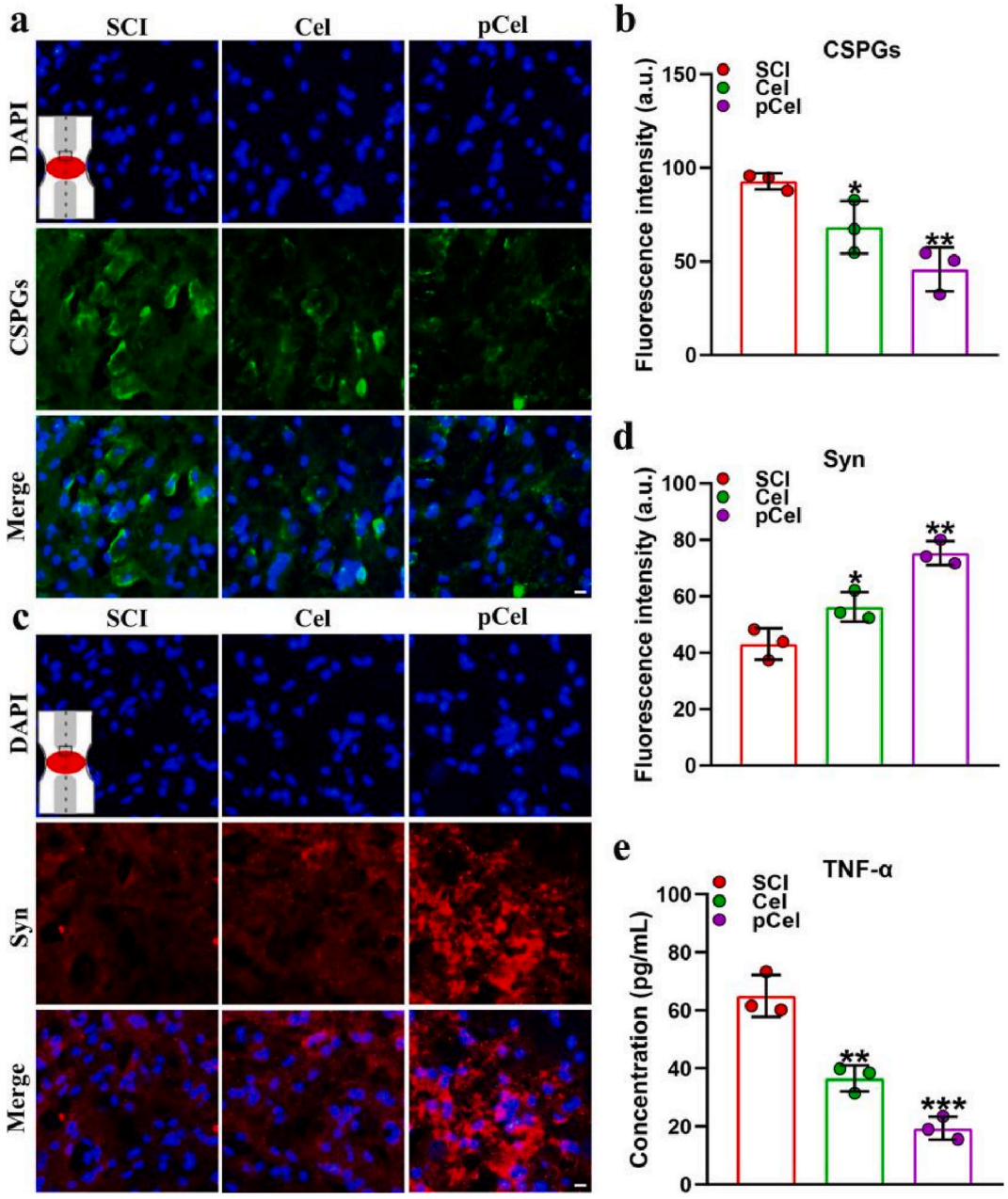

Fig. 6. In vivo synaptic regeneration and scar formation of pCel. (a) Representative images of CSPGs at the injury site. (b) Representative quantification of CSPGs at the injury site. (c) Representative images of Syn in the peripheral region. (d) Representative quantification of Synin the peripheral region. (e) Representative quantification of TNF-α in injured spinal cord. Scale bar = 10 μm *P < 0.05, **P < 0.01, compare to SCI group.

Table 1
Comparison of the motor function recovery after SCI by using different medicines.

Nanomedicines	Motor function recovery	Theraputic effects	Advantages/*Disadvantages*	Ref.
NT3-Chitosan	improve significantly	anti-infection, neuroprotection	regeneration; ***difficult to be dissolved in human fluid***	[21]
CeO_2-PCL	improve in vitro biocompatibility and auto-recovery abilities	delivered a bone regeneration drug	increases biocompatibility of the drug; ***not available for injection and the in vivo effects are unknown***	[22]
Se-CQDs	improve significantly after 8 weeks	reduced the inflammation, astrogliosis, and apoptosis induced by secondary injury	remarkable protective effect for nerves; ***not cost-effective, toxic concern***	[23]
pCel	improve significantly after 7 days	immunomodulation	reduces inflammation, injectable, low toxicity, metabolic regulation, simple preparation	current work

Note: NT3, neurotrophin3; CeO_2-PCL (CeO_2 particles assembled onto poly (ϵ-caprolactone) (PCL)) Se-CODS (Selenium-Doped Carbon Quantum Dots).

improved functional neuron regeneration, and decreased scar tissue formation. This study unraveled a novel potential for biomimetic nanoplatforms to treat CNS-related disorders, including SCI.

Credit author statement

P. Zhang and X. Mei developed the concept for this work. X. Yin and S. Lin supervised the project. Y. Xiong analyzed the data. The authors read and approved the final manuscript.

Declaration of competing interest

The authors declare that they have no known competing financial interests or personal relationships that could have appeared to influence the work reported in this paper.

Data availability

Data will be made available on request.

Acknowledgements

This work was supported by Liaoning Revitalization Talents Program (NO. XLYC1902108). All the animal experiments in this work were performed in accordance with the Ethical Committee of Care and Use of Laboratory Animals at Jinzhou Medical University.

Appendix A. Supplementary data

Supplementary data to this article can be found online at https://doi.org/10.1016/j.mtbio.2023.100836.

References

[1] C.S. Ahuja, J.R. Wilson, S. Nori, M. Kotter, C. Druschel, A. Curt, M.G. Fehlings, Traumatic spinal cord injury, Nat. Rev. Dis. Prim. 3 (2017), 17018, https://doi.org/10.1038/nrdp.2017.18.

[2] I. Eli, D.P. Lerner, Z. Ghogawala, Acute traumatic spinal cord injury, Neurol. Clin. 39 (2021) 471–488, https://doi.org/10.1016/j.ncl.2021.02.004.

[3] J.W. McDonald, C. Sadowsky, Spinal-cord injury, Lancet 359 (2002) 417–425, https://doi.org/10.1016/S0140-6736(02)07603-1.

[4] M. Canton, R. Sánchez-Rodríguez, I. Spera, F.C. Venegas, M. Favia, A. Viola, A. Castegna, Reactive oxygen species in macrophages: sources and targets, Front. Immunol. 12 (2021), 734229, https://doi.org/10.3389/fimmu.2021.734229.

[5] B. Zhang, W.M. Bailey, A.L. McVicar, J.C. Gensel, Age increases reactive oxygen species production in macrophages and potentiates oxidative damage after spinal cord injury, Neurobiol. Aging 47 (2016) 157–167, https://doi.org/10.1016/j.neurobiolaging.2016.07.029.

[6] H. Sies, V.V. Belousov, N.S. Chandel, M.J. Davies, D.P. Jones, G.E. Mann, M. P. Murphy, M. Yamamoto, C. Winterbourn, Defining roles of specific reactive oxygen species (ROS) in cell biology and physiology, Nat. Rev. Mol. Cell Biol. 23 (2022) 499–515, https://doi.org/10.1038/s41580-022-00456-z.

[7] S. Li, L. Shang, B. Xu, S. Wang, K. Gu, Q. Wu, Y. Sun, Q. Zhang, H. Yang, F. Zhang, L. Gu, T. Zhang, H. Liu, A nanozyme with photo-enhanced dual enzyme-like activities for deep pancreatic cancer therapy, Angew. Chem. 58 (2019) 12624–12631, https://doi.org/10.1002/anie.201904751.

[8] Y. Ding, Q. Pan, W. Gao, Y. Pu, K. Luo, B. He, Reactive oxygen species-upregulating nanomedicines towards enhanced cancer therapy, Biomater. Sci. (2023), https://doi.org/10.1039/d2bm01833k.

[9] F. Danhier, E. Ansorena, J.M. Silva, R. Coco, A. Le Breton, V. Préat, PLGA-based nanoparticles: an overview of biomedical applications, J. Contr. Release 161 (2012) 505–522, https://doi.org/10.1016/j.jconrel.2012.01.043.

[10] S.A. Saganuwan, Biomedical application of polymers: a case study of non-CNS drugs becoming CNS acting drugs, Cent. Nerv. Syst. Agents Med. Chem. 18 (2018) 32–38, https://doi.org/10.2174/1871524917666170821115748.

[11] Y. Zhou, Z. Peng, E.S. Seven, R.M. Leblanc, Crossing the blood-brain barrier with nanoparticles, J. Contr. Release 270 (2018) 290–303, https://doi.org/10.1016/j.jconrel.2017.12.015.

[12] Q. Chen, J. Chen, Z. Yang, J. Xu, L. Xu, C. Liang, X. Han, Z. Liu, Nanoparticle-enhanced radiotherapy to trigger robust cancer immunotherapy, Adv. Mater. (Deerfield Beach, Fla.) vol. 31 (2019), e1802228, https://doi.org/10.1002/adma.201802228.

[13] S. Maghrebi, P. Joyce, M. Jambhrunkar, N. Thomas, C.A. Prestidge, Poly(lactic-co-glycolic) acid-lipid hybrid microparticles enhance the intracellular uptake and antibacterial activity of Rifampicin, ACS Appl. Mater. Interfaces 12 (2020) 8030–8039, https://doi.org/10.1021/acsami.9b22991.

[14] S.R. Chen, Y. Dai, J. Zhao, L. Lin, Y. Wang, Y. Wang, A mechanistic overview of Triptolide and celastrol, natural products from Tripterygium wilfordii hook F, Front. Pharmacol. 9 (2018) 104, https://doi.org/10.3389/fphar.2018.00104.

[15] L. Guo, Y. Zhang, K.T. Al-Jamal, Recent progress in nanotechnology-based drug carriers for celastrol delivery, Biomater. Sci. 9 (2021) 6355–6380, https://doi.org/10.1039/d1bm00639h.

[16] S. Xu, Y. Feng, W. He, W. Xu, W. Xu, H. Yang, X. Li, Celastrol in metabolic diseases: progress and application prospects, Pharmacol. Res. 167 (2021), 105572, https://doi.org/10.1016/j.phrs.2021.105572.

[17] A.C. Allison, R. Cacabelos, V.R. Lombardi, X.A. Alvarez, C. Vigo, Celastrol, a potent antioxidant and anti-inflammatory drug, as a possible treatment for Alzheimer's disease, Prog. Neuro-Psychopharmacol. Biol. Psychiatry 25 (2001) 1341–1357, https://doi.org/10.1016/s0278-5846(01)00192-0.

[18] T.H. Hutson, S. Di Giovanni, The translational landscape in spinal cord injury: focus on neuroplasticity and regeneration, Nat. Rev. Neurol. 15 (2019) 732–745, https://doi.org/10.1038/s41582-019-0280-3.

[19] W. Young, Spinal cord regeneration, Cell Transplant. 23 (2014) 573–611, https://doi.org/10.3727/096368914X678427.

[20] P.A. Lim, A.M. Tow, Recovery and regeneration after spinal cord injury: a review and summary of recent literature, Ann. Acad. Med. Singapore 36 (2007) 49–57.

[21] J.S. Rao, C. Zhao, A. Zhang, H. Duan, P. Hao, R.H. Wei, J. Shang, W. Zhao, Z. Liu, J. Yu, K.S. Fan, Z. Tian, Q. He, W. Song, Z. Yang, Y.E. Sun, X. Li, NT3-chitosan enables de novo regeneration and functional recovery in monkeys after spinal cord injury, Proc. Natl. Acad. Sci. U.S.A. 115 (2018) E5595–E5604, https://doi.org/10.1073/pnas.1804735115.

[22] L. Dong, X. Kang, Q. Ma, Z. Xu, H. Sun, D. Hao, X. Chen, Novel approach for efficient recovery for spinal cord injury repair via biofabricated nano-cerium oxide loaded PCL with Resveratrol to improve in vitro biocompatibility and autorecovery abilities, Dose Response 18 (2020), 1559325820933518, https://doi.org/10.1177/1559325820933518.

[23] W. Luo, Y. Wang, F. Lin, Y. Liu, R. Gu, W. Liu, C. Xiao, Selenium-doped Carbon Quantum Dots efficiently ameliorate secondary spinal cord injury via scavenging reactive oxygen species, Int. J. Nanomed. 15 (2020) 10113–10125, https://doi.org/10.2147/IJN.S282985.